

# Thermal Effects on Wellbore Stability and Fluid Loss in High-Temperature Geothermal Drilling

Mubarek Alpkiray; Tan C. Nguyen, New Mexico Tech; Arild Saasen, University of Stavenger

Copyright 2022, AADE

This paper was prepared for presentation at the 2022 AADE Fluids Technical Conference and Exhibition held at the Marriott Marquis, Houston, Texas, April 19-20, 2022. This conference is sponsored by the American Association of Drilling Engineers. The information presented in this paper does not reflect any position, claim or endorsement made or implied by the American Association of Drilling Engineers, their officers or members. Questions concerning the content of this paper should be directed to the individual(s) listed as author(s) of this work.

## Abstract

Geothermal drilling operations contain numerous challenges that are encountered to increase the well cost and non-productive time. Fluid loss is one of the key issues that can cause well abandonment in geothermal drilling. Lost circulation can be seen due to naturally fractures, high mud weight, and extremely high formation temperatures. This challenge may cause wellbore stability problems and lead to expensive drilling operations. Wellbore stability is the main domain that should be considered to mitigate or prevent fluid loss into the formation. This paper describes the causes of fluid loss in the Pamukoren geothermal field in Turkey. A geomechanics approach integration and assessment is applied to help the understanding of fluid loss problems. In geothermal drilling, geomechanics is primarily based on rock properties, in-situ stress characterization, the temperature of the rock, determination of stresses around the wellbore, and rock failure criteria. Since a high-temperature difference between the wellbore wall and drilling fluid is presented, temperature distribution through the wellbore is estimated and implemented to the wellbore stability approach. This study reviewed geothermal drilling data to analyze temperature estimation along the wellbore, the cause of fluid loss, and stored electric capacity of the reservoir. Our observation demonstrates the geomechanical approach's significance role in understanding the safe drilling operations on high-temperature wells. Fluid loss is encountered due to thermal stress effects around the borehole. This paper provides a wellbore stability analysis for a geothermal drilling operation to discuss the causes of lost circulation resulting in nonproductive time and cost.

## Introduction

Geothermal energy is the heat energy generated from the world crust by processing hot water or steam in extremely hot temperatures. Geothermal energy is harnessed to generate clean energy in hot or medium temperature reservoir resources that present close to tectonic plates. It is noted that a significant pro of geothermal energy that weather conditions do not impact generating energy. Since it has long-term process capability,

geothermal energy is generated consistently, running 24 hours per day. It can also be harnessed for energy production without importing fuel. Due to the many advantages of geothermal energy, governments and companies have embarked on releasing new investments to clean geothermal energy in the last two decades.

Geothermal energy covers almost the same drilling operations in oil and gas drilling technology. Geothermal drillings can be operated either in shallow depths or deep wells, depending on the resource temperature. Since high temperature is considered while drilling, geothermal operations costs correspond to increase expenditures and possible drilling challenges. Many problems can be seen in geothermal drilling, such as wellbore stability, lost circulation, and corrosivity leads to economic difficulty due to types of formations encountered in geothermal drilling.

One of the challenges in geothermal drilling is fluid loss. Drilling fluid has the ability to transport cuttings, maintain a proper hydrostatic pressure against pore pressure and cool the bit. The drilling fluid is prepared depending on the depth, pore pressure, and temperature of the bottomhole. Alteration of drilling mud can cause either drilling induced-tensile fracture or breakout failure. While increasing mud weight can cause fluid loss into the formation, decreasing the mud weight leads to shear failure around the borehole. Lost circulation is defined as the losing fluid into fractures, cavernous and high-permeability formations. The loss is determined based on the amount of drilling fluid barrels per hour. There are encountered different types of losses, such as seepage (less than 25 barrels per hour), partial (25-100 barrels per hour), and severe (higher than 100 barrels per hour). If there is no presence of the mud at surface, it is called total loss. Drilling can only be maintained under total loss conditions before 50 ft depth of the next casing running (Cole et al., 2017). The problem with the total loss condition is that the driller cannot control hydrostatic pressure in overbalance drilling for unpredicted bottomhole conditions. Besides, the temperature is another function to cause fluid loss phenomena. Since the mud temperature is cooler than the bottomhole wellbore wall, the cooling effect leads to solid

shrinkage and stress relaxation on the formation (Espinoza, 2020). This depends on the temperature difference between the wall and fluid.

Once the lost circulation is encountered, several actions can be applied. However, some steps should be monitored to prevent or predict fluid loss, such as mud weight and temperature, pore pressure and temperature, and cuttings loading. Maintaining a proper bottomhole pressure is a crucial action to avoid fluid loss into the formation. Geomechanics research has an important role in monitoring wellbore stability during geothermal drilling operations. Wellbore stability consideration means controlling the lower and upper bound of the mud window to achieve a more stable well. In geothermal drilling, lost circulation can occur due to high mud pressure or temperature differences. The temperature is also considered to result in fluid loss while drilling a geothermal well. The concentration of stress around the wellbore should be analyzed to show whether the failure is present or not. Stresses around the wellbore are a function of far-field stress magnitudes as considered vertical and two horizontal stresses. Applying thermal effects on stresses in the borehole assists in observing a clear idea about lost circulation phenomena in high-temperature reservoir rocks by implementing a failure criteria. This paper identifies the leading causes of fluid loss in geothermal drilling and presents geomechanical applications to prevent the challenge.

### Stresses Around a Wellbore

While drilling a circular well, the new well creates a new rock surface and stress concentration on the wellbore wall, as shown in Fig. 1. As cuttings are removed from the well, the wellbore wall becomes more unstable, and far-field stresses are no longer supported and considered. Compressive stress increases at the direction of minimum horizontal stress and decreases at the direction of maximum horizontal stress. While raising compressive stress results in breakouts, reducing it leads to tensile failure of the borehole wall (Zoback, 2010). Therefore, the stress magnitude in a drilled vertical well based on an isotropic and elastic medium can be predicted by applying Kirsch equations (Kirsch, 1898; Jaeger et al., 2009). The effective stresses around a vertical wellbore can be predicted by the following equations (Zoback, 2010):

$$\begin{aligned} \sigma_{rr} = & \frac{1}{2}(S_{Hmax} + S_{hmin} - 2P_p) \left(1 - \frac{a^2}{r^2}\right) \\ & + \frac{1}{2}(S_{Hmax} - S_{hmin}) \left(1 - \frac{4a^2}{r^2} \right. \\ & \left. + \frac{3a^4}{r^4}\right) \cos 2\theta + \frac{a^2}{r^2}(P_w - P_p) \end{aligned} \quad (1)$$

$$\sigma_{\theta\theta} = \frac{1}{2}(S_{Hmax} + S_{hmin} - 2P_p) \left(1 + \frac{a^2}{r^2}\right) \quad (2)$$

$$\begin{aligned} & - \frac{1}{2}(S_{Hmax} - S_{hmin}) \left(1 \right. \\ & \left. + \frac{3a^4}{r^4}\right) \cos 2\theta - \frac{a^2}{r^2}(P_w - P_p) \\ & - \sigma^{\Delta T} \end{aligned}$$

$$\sigma_{zz} = S_v - 2\nu(S_{Hmax} - S_{hmin}) \frac{a^2}{r^2} \cos 2\theta - P_p \quad (3)$$

$$- \sigma^{\Delta T}$$

$$\tau_{r\theta} = \frac{1}{2}(S_{Hmax} - S_{hmin}) \left(1 + \frac{2a^2}{r^2} \right. \quad (4)$$

$$\left. - \frac{3a^4}{r^4}\right) \sin 2\theta$$

where  $\sigma_{rr}$ ,  $\sigma_{\theta\theta}$  and  $\sigma_{zz}$  are effective radial, tangential, and axial stresses, respectively;  $S_v$  is vertical stress,  $S_{Hmax}$  is maximum horizontal stress,  $S_{hmin}$  is minimum horizontal stress,  $P_p$  is the formation of pore pressure,  $P_w$  is the mud pressure,  $\nu$  is Poisson's ratio,  $\theta$  is the angle between the direction of maximum horizontal stress and the direction at which stress is considered,  $\sigma^{\Delta T}$  is thermal stress from the difference between formation temperature and mud temperature.

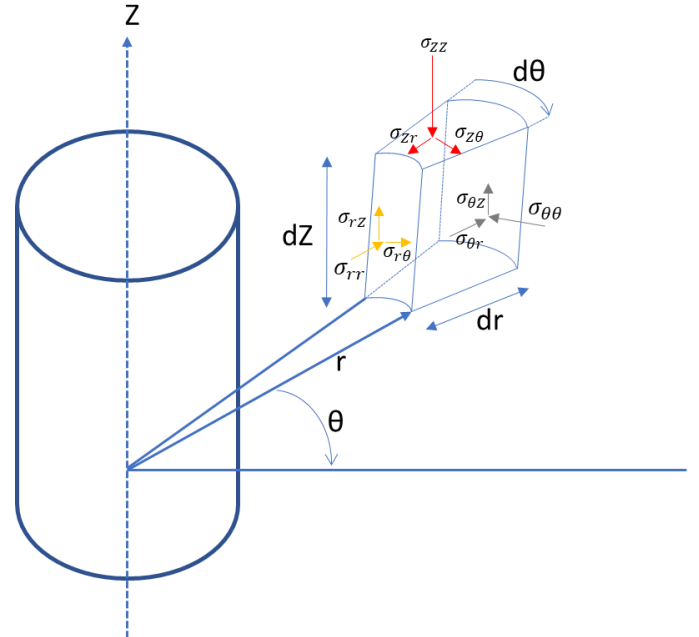


Figure 1. Stress distribution around the wellbore.

Considering wellbore wall conditions ( $r = a$ ) can help better analyze either breakouts or drilling-induced tensile fractures. Since axial stress acts parallel to the wellbore axis (not a function of bottomhole pressure and pore pressure), it is not considered to observe failures. Therefore, effective radial and hoop stresses at the wellbore wall are expressed as follows:

$$\sigma_{rr} = (P_w - P_p) \quad (5)$$

$$\sigma_{\theta\theta} = (S_{Hmax} + S_{hmin} - 2P_p) - (S_{Hmax} - S_{hmin}) \cos 2\theta - (P_w - P_p) - \sigma^{\Delta T} \quad (6)$$

Since hoop stress is a function of  $\theta$  angle, it varies with depending on the direction of minimum ( $0^\circ$  and  $180^\circ$ ), and maximum ( $90^\circ$  and  $270^\circ$ ) compression as given follows:

$$\sigma_{\theta\theta}^{min} = 3S_{hmin} - S_{Hmax} - 2P_p - \Delta P - \sigma^{\Delta T} \quad (7)$$

$$\sigma_{\theta\theta}^{max} = 3S_{Hmax} - S_{hmin} - 2P_p - \Delta P - \sigma^{\Delta T} \quad (8)$$

where  $\Delta P$  is the difference between formation pore pressure and mud pressure.

### Thermal Stress Effects on Lost Circulation Phenomena

Once the temperature between the mud and wellbore is higher than expected, the additional stress term is added to the stresses around the wellbore. The temperature effect differences on thermal stress can be either compressive or tensile depending on higher or lower than normal temperature gradient. The presence of cooler mud temperature than the formation rock temperature is the possibility of encountering tensile thermal stress conditions around the borehole. In geothermal drilling, the drilling fluid is usually cooler than the wellbore wall temperature. This cooling effect causes that the formation starts contracting, resulting in tensile stress. The cooling effect is time-dependent; the more contact between the fluid and the wellbore wall results in more temperature changes as going far away from the borehole. Therefore, with increasing time, the higher the likelihood of increasing the tensile stresses leading to fluid loss problems. On the contrary, the cooling effect helps to mitigate the borehole against collapse. Cooling down the bottomhole causes solid shrinkage and stress relaxation reducing compressive stress (Espinoza, 2020).

Thermal stresses vary based on formation rock properties and temperature differences such as the rock wall temperature, Elastic Young's modulus, thermal expansion coefficient, Poisson's ratio, and circulated fluid temperature as expressed in Eq. 9 (Fjær et al., 2008; Turcotte & Schubert, 2002; Zoback, 2010). If the temperature differences are not high, thermal stresses can be neglected (Zoback, 2010); thereby, mud weight has more impact on stability. However, thermal stress effects should be considered in geothermal well drillings due to lower mud temperature and higher wall temperature. If thermal stress leads to exceeding the rock tensile strength, lost circulation will occur.

$$\sigma^{\Delta T} = \frac{\alpha_t E \Delta T}{1 - \nu} \quad (9)$$

where  $\alpha_t$  is the thermal expansion coefficient of the rock ( $1/^\circ\text{F}$ ),  $E$  is Elastic Young's modulus (psi),  $\nu$  is Poisson's ratio (frac),  $\Delta T$  is the temperature difference between wellbore wall and drilling fluid ( $^\circ\text{F}$ ).

Lost circulation is outlined as loss of drilling mud to pores or fractures. It is one of the costly challenges often encountered

in geothermal drilling and one of the primary contributors to non-productive time while drilling. Lost circulation can result in additional costs due to lost circulation materials, time, and other wellbore problems. Fluid loss accounts for 10% of total well costs in geothermal wells (Carson & Lin, 1982). While drilling, fluid loss is encountered in highly permeable zones and naturally or induced fractured formations. Numerous factors cause drilling loss, such as poor drilling practices or types of formations drilling into (Shaker Selim, 2008). It is noted that the hydrostatic pressure during drilling operations is maintained greater than formation pressure to avoid well control issues. While lost circulation encountered, many geothermal wells have been abandoned, putting the project into economic difficulty (Cole et al., 2017). If curing the loss action is not taken into consideration immediately, the amount of loss and fracture width will increase.

When lost circulation is encountered, several methods can be implemented to cure or mitigate fluid loss, such as controlling drilling mud weight, using lost circulation materials (LCM), and monitoring drilling mud temperature. To mitigate or avoid fluid loss events a series best practices can be implemented to successfully drill and complete geothermal wells such as preparing a convenient well planning and design as well as based on organization and communication between well-educated drilling crew. Geomechanics is one of the approaches applied to analyze thermal effects, wellbore instability, and mud weight.

### Mohr-Coulomb Failure Criterion

One of the most commonly applied failure criteria is Mohr-Coulomb among geomechanics applications. While the triaxial test is used for linear Mohr-Coulomb failure criteria, the polyaxial test is more applicable for a non-linear form of failure criteria due to more accurate results. The criterion consists of the Mohr circle and Coulomb failure envelope. The circle represents the stress magnitudes such as greatest, least, and shear. Coulomb envelope corresponds to determine whether the failure occurs due to contact between line and circle (Al-Ajmi & Zimmerman, 2005). Also, the Coulomb line is based on the shear failure plane because of the effect of shear stress on that plane. Mohr-Coulomb can be drawn for either in 2D or 3D plane, and it assumes that intermediate stress does not influence rock strength.

Failure envelope is a function of the internal friction of rock, the normal stress component, and the rock cohesion as expressed in Eq. 10. Cohesion changes based on the stiffness of rock. While hard formation rocks tend to present a higher cohesion value, soft rocks have a low magnitude of cohesion (Zoback, 2010). The Mohr-Coulomb failure criterion can be presented with the greatest and the least principal stresses in Eq. 12.

$$\tau = c + \mu \sigma \quad (10)$$

$$\mu = \tan \varphi \quad (11)$$

$$\sigma_1 = C_0 + q \sigma_3 \quad (12)$$

where  $\tau$  is normal shear stress (psi),  $\sigma$  is normal stress (psi),  $c$  is the cohesion of the rock (psi),  $\mu$  is the internal friction coefficient,  $\varphi$  is friction angle (deg.),  $q$  is flow factor,  $\sigma_1$  and  $\sigma_3$  are maximum and minimum stresses, respectively.

Mohr-Coulomb diagram helps to estimate optimum mud windows for drilling operations. To implement failure criteria into wellbore stability, wellbore stresses around the borehole are considered for the tensile rock failure. The least principal stress ( $\sigma_3$ ) is similar to radial stress ( $\sigma_{rr}$ ) which is the difference between mud weight and pore pressure under overbalance drilling conditions. Since the hoop stress is considered a circumferential stress perpendicular to the axial direction, it is considered the greatest stress in the failure plot, as expressed in

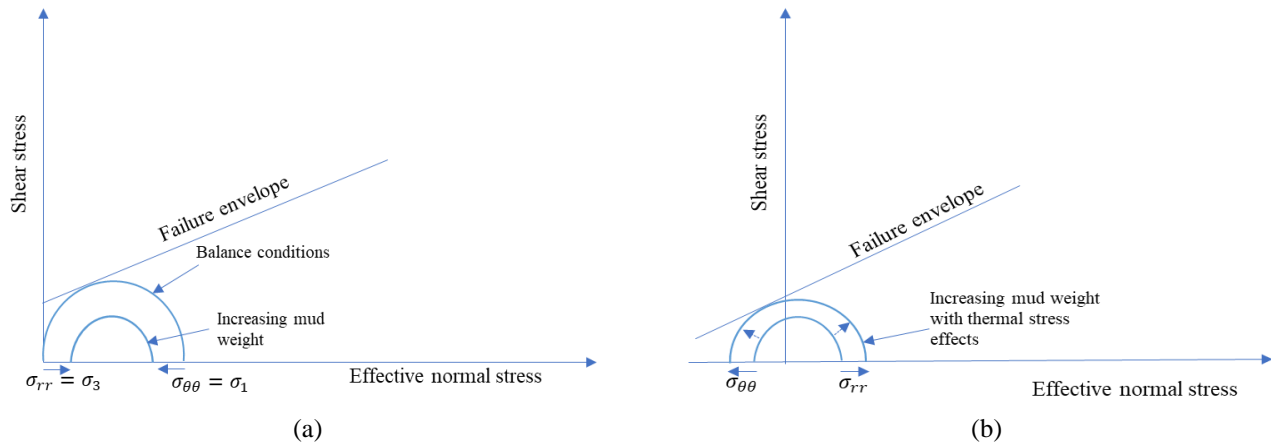


Figure 2. (a) wellbore balance condition ( $\sigma_{rr} = P_w - P_p = 0$ ) and increasing mud weight. (b) Increasing mud weight with thermal effects conditions resulting leading the possibility of tensile failure.

### Heat Transfer Through Wellbore

Wellbore instability usually occurs in high-temperature differences between formation wall and fluid temperature in geothermal drilling operations. Thermal stress significantly affects the enlargement of induced-tensile fractures (Loeppeke et al., 1990). While drilling mud cools down the well, formation rocks lead to reducing the rock strength due to temperature differences resulting in loss from the well to the formation. Therefore, it is necessary to predict drilling fluid estimation through wellbore in Fig. 3. Due to rapid temperature changes, the heat exchange between wall and mud is an unstable heat-transfer state.

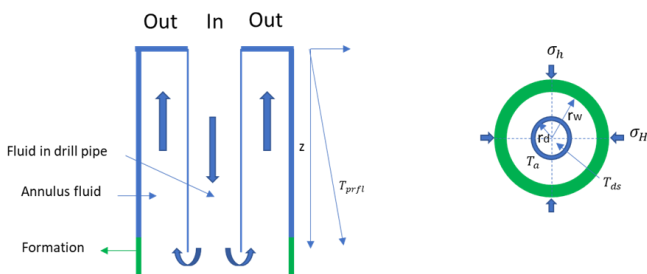


Figure 3. Temperature profile distribution through the wellbore.

Fig. 2. Once the mud weight is equal to pore pressure ( $\sigma_{rr} = P_w - P_p = 0$ ), wellbore failure might occur without a high magnitude of hoop stress (Zoback et al., 2003). However, raising mud weight or hydrostatic pressure increases radial stresses and a decrease in hoop stresses, as presented in Eq. 5-6. Note that a sufficient enhancement of mud weight with thermal stress effects causes the occurrence of tensile conditions in hoop stress. If hoop stress value exceeds the tensile strength of the rock, there is a possibility to present fluid loss into formation.

There have been proposed numerous temperature distributions through wellbore during drilling operations. Most of the approaches were based on transient flow, which requests detailed drilling history. One of the most known first numerical analyses was observed by Raymond (Raymond, 1969), including unsteady and pseudo-steady-state conditions with multiple casing strings. This approach aims to overcome unsteady-state conditions for heat exchange problems. Besides, Holmes and Swift (Holmes & Swift, 1970), Kabir et al. (Kabir et al., 1996), and Hasan et al. (Hasan & Kabir, 1994) developed analytical solutions and present more uncomplicated solutions considering forward or reverse circulations. Validations for the analytical approach was applied when drilling data was analyzed.

Conversion of energy is based on the presence of temperature differences, as expressed in Fig. 4. Energy transfer in a wellbore can be either conductive or convective. Conductive heat transfer is the heat exchange from the higher temperature formation to the cooler wellbore and between the inside drillstring and annulus. Convective heat exchange accounts for heat transfer of the drilling fluid itself. In academia, there have been developed two different approaches to determine heat transfer type. While some studies proposed that the heat exchange direction is from the wellbore to the

formation, others observed that heat transfer can be seen from the initial formation temperature toward the wellbore. The obtained total amount of heat is the difference between these two approaches.

Energy transfer occurs after a hole is drilled either from the reservoir into the wellbore or from the annulus into the drill pipe. The model considers the energy balance between formation-annulus and the annulus-drillstring in Fig. 4. While the temperature distribution inside the wellbore is based on the assumption of steady-state heat flow, formation heat exchange is a function of transient heat conduction adopted from Al-Saedi (Al Saedi, 2020). The heat transfer calculations in the annulus are as follows:

$$Q_{a(z+dz)} - Q_{a(z)} = Q_{ads} - Q_{FW} \quad (13)$$

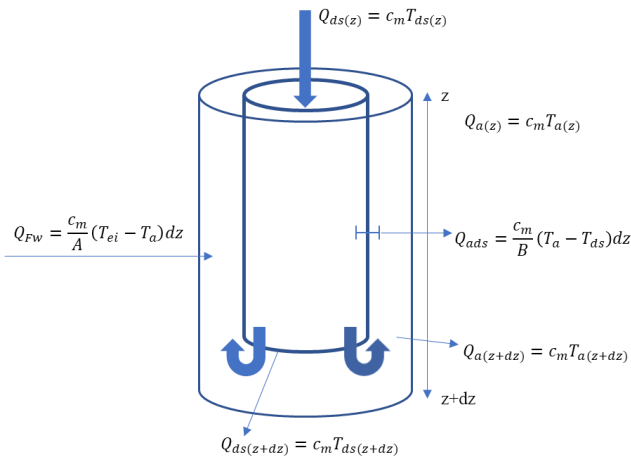


Figure 4. Heat energy transfer between the wellbore and drill string considering forward circulation.

Since there is no difference between the heat flow from formation to the wellbore and the heat flow from the wellbore to the annulus, the temperature of the wellbore wall is equal to the temperature of the annulus ( $T_{wb} = T_a$ ). In addition, the heat

flow from the annulus to the drilling string is expressed as follows:

$$Q_{ads} = \frac{c_m}{B} (T_a - T_{ds}) dz \quad (14)$$

The result for temperature distribution equations is expressed as given below:

$$T_{ds} = \gamma e^{\xi_1 z} + \delta e^{\xi_2 z} + g_G Z - B g_G + T_{es} \quad (15)$$

$$T_a = (1 + \xi_1 B) \gamma e^{\xi_1 z} + (1 + \xi_2 B) \delta e^{\xi_2 z} + g_G Z + T_{es} \quad (16)$$

where,  $T_{ds}$  and  $T_a$  the temperature inside drill string and annulus respectively;  $Z$  is the reference depth  $g_G$  is the geothermal gradient ( $^{\circ}\text{F}/\text{ft}$ ),  $\xi_1$  and  $\xi_2$  were developed as constants depending on thermal properties,  $\gamma$  and  $\delta$  are constants for boundary conditions (Al Saedi, 2020).

## Result and Discussion

Field data from a well located in Turkey was obtained to observe thermal effects on wellbore instability during fluid loss events. The data was provided by the General Directorate of Mineral Research and Exploration (MTA). Available data is drilling operations parameters, rock formation properties, production rate, and completion. PML1 well is located in the western part of Turkey from Pamukoren geothermal field. The field is mainly based on faults forming of Buyuk Menderes Graben. Since geothermal wells present the temperature differences between fluid and wellbore wall, temperature distribution through wellbore should be predicted to obtain more accurate bottomhole conditions.

### Temperature Distribution Along the Wellbore

This section applies data from a case study to observe temperature distribution through the wellbore, stresses around the wellbore, and failure criterion. The guideline used in the following computations for temperature distribution is presented in Table 1.

Table 1. Used parameters for temperature prediction.

Parameter	Notation	Value	Field Unit	Value	SI Unit
Total vertical depth	TVD	3444	ft	1050	m
Circulation flow rate	w	17000	lbm/h	34	gpm
Drill-string radius	$r_t$	5 2/5	in	0.14	m
Wellbore radius	$r_e, r_w$	8 1/2	in	0.22	m
Casing inner radius	$r_c$	7	in	0.18	m
Fluid loss depth	z	3050	ft	930	m
Formation density	$\rho_e$	165	lbm/ft <sup>3</sup>	2643	kg/m <sup>3</sup>
Mud density	$\rho_m$	9.6	lbm/gal	1150	kg/m <sup>3</sup>
Surface temperature	$T_{es}$	77	$^{\circ}\text{F}$	25	$^{\circ}\text{C}$ .
Mud specific heat capacity	$C_{fl}$	0.54	Btu/lbm- $^{\circ}\text{F}$	2260	J/kg- $^{\circ}\text{C}$ .
Formation specific heat capacity	$c_e$	0.2	Btu/lbm- $^{\circ}\text{F}$	837	J/kg- $^{\circ}\text{C}$ .
Formation thermal conductivity	$k_r$	1.2-1.7	Btu/ft-hr- $^{\circ}\text{F}$	2.07-2.94	W/m- $^{\circ}\text{C}$ .
Mud thermal conductivity	$k_f$	0.55	Btu/ft-hr- $^{\circ}\text{F}$	0.95	W/m- $^{\circ}\text{C}$ .
Earth thermal conductivity	$k_e$	0.867	Btu/ft-hr- $^{\circ}\text{F}$	1.5	W/m- $^{\circ}\text{C}$ .
Drill-pipe thermal conductivity	$k_{dp}$	25	Btu/ft-hr- $^{\circ}\text{F}$	43.2	W/m- $^{\circ}\text{C}$ .
Geothermal gradient	$g_G$	0.092	$^{\circ}\text{F}/\text{ft}$	0.17	$^{\circ}\text{C}/\text{m}$

Since geothermal drilling is considered thermal stress effects, there should be estimated temperature at the bottomhole. The temperature distribution during drilling in drillstring and annulus can be obtained by using Eq. 15-16. Validation of the model is based on using drilling survey temperature values.

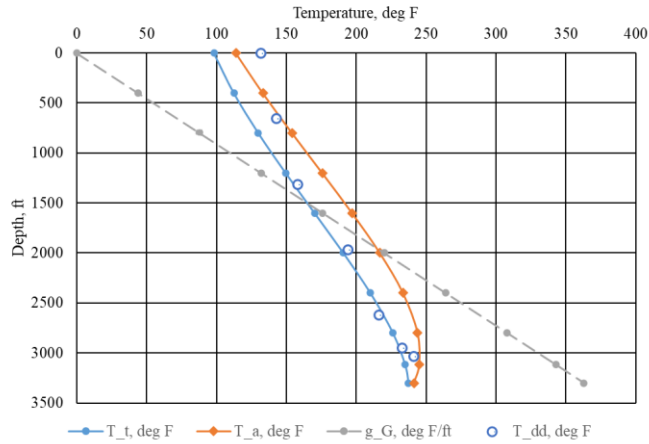


Figure 5. Fluid temperature distribution estimation in

Table 2. Mechanical wellbore analysis parameters.

Parameters	Notation	Value	Unit	Value	SI Unit
Depth	$z$	3050	ft	930	m
Porosity	$\phi$	0.07	-	0.07	-
Elastic Young's modulus	$E$	7.8E+06	psi	53E+0.3	MPa
Poisson's ratio	$\nu$	0.25	-	0.25	-
Pore pressure	$P_p$	1320	psi	9.1	MPa
Bottomhole pressure	$P_{bhp}$	1634	psi	11.2	MPa
Vertical stress	$S_v$	3867	psi	26.6	MPa
Maximum horizontal stress	$S_H$	2667	psi	18.3	MPa
Minimum horizontal stress	$S_h$	2169	psi	14.9	MPa
Thermal expansion coefficient	$\beta$	1.84E-06	1/°F	3.31E-06	1/°C.
Wellbore radius	$r$	0.58	ft	0.22	m
Wellbore wall temperature	$T_w$	330	°F	165	°C.
Mud temperature	$T_m$	245	°F	118	°C.

Thermal stress is affected by the temperature differences between wellbore wall and fluid, elastic modulus, thermal expansion coefficient, and Poisson's ratio. The variation of thermal stress based on temperature differences was used to calculate the alteration of stresses around the wellbore. The lower temperature of the fluid leads to a reduction in hoop stress and enhancement in thermal stress in Fig. 6. It is observed that the wellbore fluid temperature varies from 206 °F to 266 °F because changing mud rate causes changes in drilling fluid temperature. If higher mud circulation is presented, the mud temperature at the bottomhole conditions is reduced and the temperature differences increase as expressed in Fig. 7. This demonstrates that temperature is a necessary component to consider in geothermal drilling. Radial stress is a function of the difference between hydrostatic pressure and pore pressure; therefore, there is no change. The only parameter that can

annulus and drilling pipe.

Fig. 5 shows the temperature in drillstring ( $T_t$ ), annulus ( $T_a$ ), drilling data ( $T_{dd}$ ), and geothermal gradient ( $g_G$ ). It can be seen that there are temperature differences between the annulus and inside drill pipe because annulus fluid has direct contact with the wellbore wall causing more heat transfer. Another reason for temperature differences is that geothermal drilling pipes are usually manufactured to be more insulated than conventional drill pipes. Hence, geothermal drilling pipes are less conductive. The model temperature tends to be matched by increasing depth due to the average thermal conductivity of formation rocks and materials.

### Wellbore Stress Estimation with Thermal Effect

After analyzing the temperature profile along the wellbore, thermal impacts on wellbore stability can be implemented using a geomechanics approach to identify wellbore failure. To determine the fluid loss in the well, rock and thermal properties, stress magnitudes, well data from the field were used. Thermal properties are mainly based on typical values. Since there are not presented comprehensive well data, maximum horizontal stress is assumed to be between vertical and minimum horizontal stresses. General inputs for sensitivity analysis are given in Table 2.

change radial stress is the increase or decrease mud weight. To maintain mud weight below pore pressure magnitude might result in breakout condition causing stuck pipe problem. Also, a sufficient increase in mud density can lead to higher radial stress and lower hoop stress.

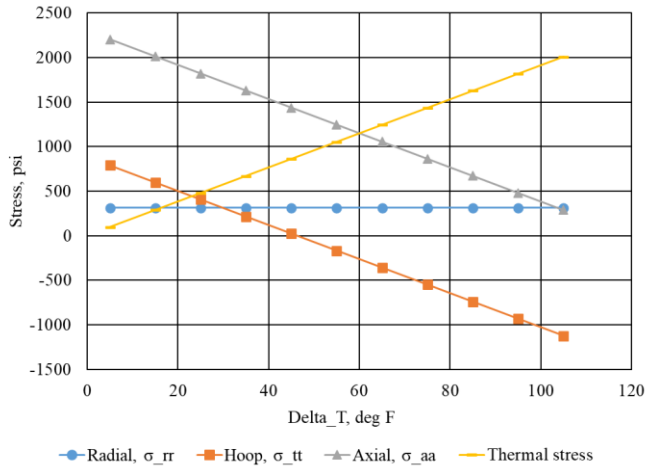


Figure 6. Thermal stress variation on wellbore stresses at  $S_{hmax}$  direction.

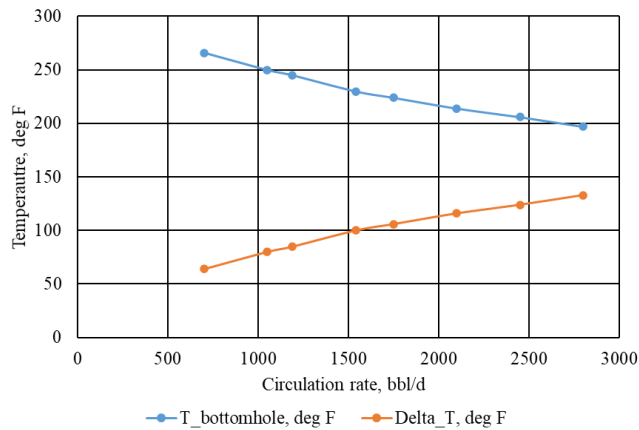
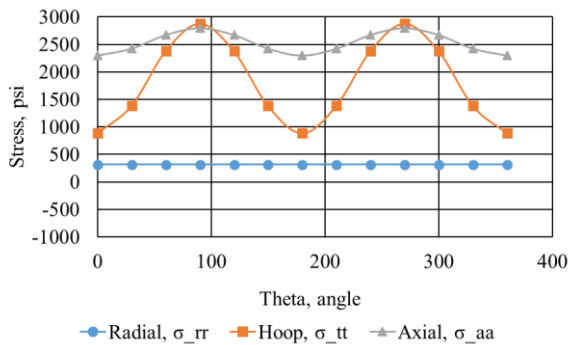
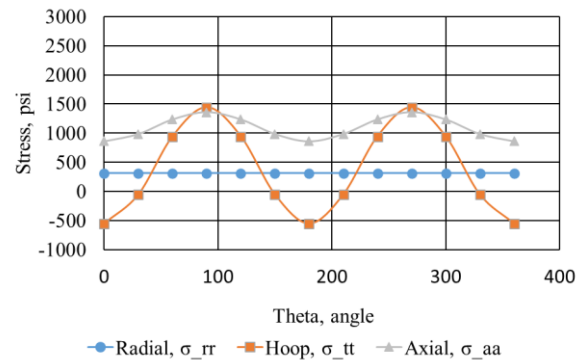


Figure 7. Mud circulation rate effect on fluid temperature.

Surface temperature is another factor that can vary with weather conditions such as winter and summer time. The drilling field location has an average of 50 °F for wintertime and 100 °F for summertime. Fig. 8 shows the drilling bottomhole temperature changes based on different surface temperature



(a)



(b)

Figure 9. (a) Stresses around the wellbore without temperature consideration. (b) Temperature effects on wellbore stresses.

conditions. There is seen a noticeable alteration if drilling operations are maintained either in cold or hot weather. In particular, cold weather might cause higher temperature differences than hot surface weather. This may present higher tensile hoop stress magnitudes resulting in a possible high amount of fluid loss into the formation.

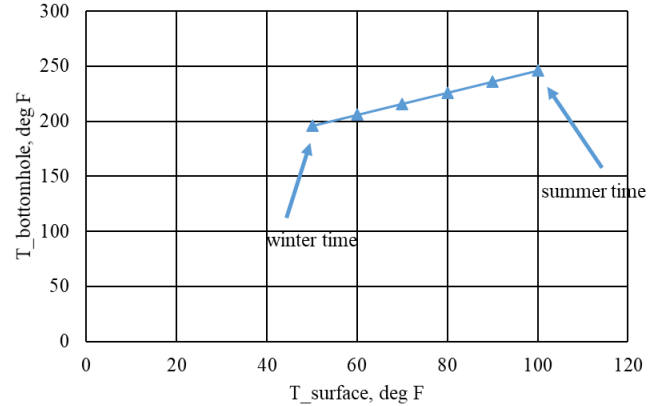


Figure 8. Surface temperature effects on bottomhole temperature.

Calculations based on Eq. 5-8 show that the hoop stress varies with angle and horizontal stresses while radial stress is constant. Since axial stress is primarily a function of overburden, there is no consideration for failure. Fig. 9 shows the demonstration of variation of stresses around borehole (0° and 180° angle) without thermal (a) and with thermal (b) effects at the same depth. It is considered thermal effects on geothermal drilling because the high-temperature differences are presented. It can be clearly seen that hoop (or tangential) and axial stresses rapidly reduce due to the temperature differences between the wellbore wall (330 °F) and fluid (245 °F). The meaning of negative hoop stress is that there is a possibility of fluid loss into the formation. If its value exceeds the strength of the rock ( $-T_0$ ), tensile failure may happen.

**Effect of Temperature on Rock Failures**

Mohr-Coulomb criteria is the most commonly used failure criteria in the industry. Once the stress values are implemented into failure criteria, radial and hoop stresses can show the failure as presented in Fig. 10. These results show that consideration of thermal stress impacts can be plotted in Mohr-Coulomb failure criteria. The figure explains that the tensile failure represents fluid loss during drilling operations due to the temperature factor. The circle on the right represents without temperature effects. Once the temperature is considered, the circle moves toward the left side, resulting in a negative circumferential stress value.

Coulomb envelope can be obtained by using Eq. 10 as a function of cohesion, normal stress, and the internal friction coefficient. This study uses an experimental study of marble rock by proposed Handin and Hager (Handin & Hager, 1957). The values of cohesion and internal friction coefficient are 1151 psi and 0.22 frac., respectively.

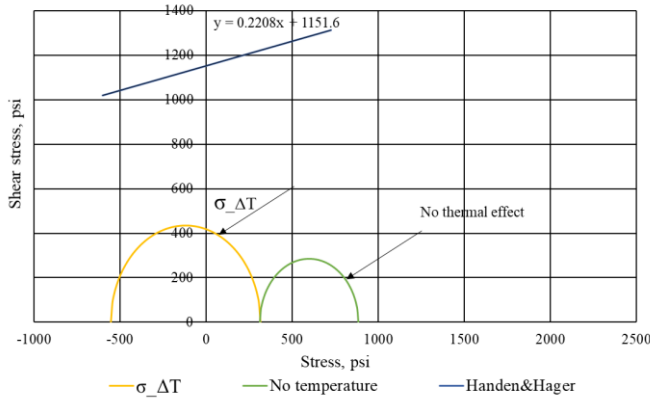


Figure 10. Integrating wellbore stresses into Mohr-Coulomb failure criterion.

Comparing near-well temperature and stress alteration is observed and is focused on plotting failure conditions with varying temperatures. The different temperature values were analyzed based on fluid temperature and thermal stress and plotted on Mohr-Coulomb failure criteria in Fig. 11. The lower mud temperature results in increasing the temperature differences between mud and the wellbore wall. This is called the cooling effect causing more fluid loss or severe conditions. Since hoop stress is considered to interpret whether there is a failure or not, tension failure it is likely to occur (fluid loss) in low fluid temperature conditions if the hoop stress value exceeds the tensile strength of the rock.

Mohr-Coulomb diagram shows using hoop and radial stress at different fluid temperature conditions to indicate changes in wellbore stability at different circulation rates. Higher temperature differences result in a lower tangential stress value causing drilling fluid loss. The presence of tensile thermal stresses by cooling effect can lead to fracture formation or enhance the propagation of existing fractures in geothermal drilling. Therefore, the effects of thermal stress on the wellbore wall present loss of circulation phenomena and reduce the

magnitude of hoop stress acting on the wellbore wall.

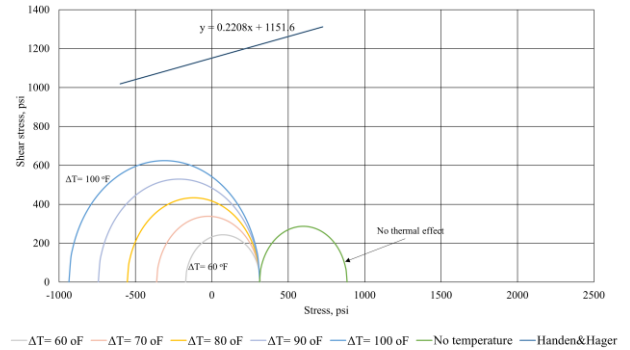


Figure 11. Effect of variation of temperature differences.

Our study demonstrates that the high-temperature differences in a geothermal well might cause severe fluid loss. The effect of cooling wellbore wall based on drilling mud shows that the temperature difference higher than 100 °F is the reason for more severe tensile failure occurrence by observing filed data. Drilling report explains that after encountering fluid loss scenarios, there was not fluid flow at the surface, which shows the total lost circulation. The amount of fluid loss was more than 7500 barrels of mud in 15 days. It is observed that lost circulation leads to high non-productive time and cost. Since the fluid loss formation was 400 ft above the reservoir, there was not taken any precaution to cure loss formation by applying lost circulation materials.

Hoop stress is considered to identify tensile failure or fluid loss. The PML1 well analysis indicates that the hoop stress value of around -900 psi can be a reasonable effect to encounter total fluid loss. These results show that the lower tensile values might cause lost circulation; however, the loss may not be severe, or it can be partial or seepage fluid loss.

**Rock Properties Effects**

More calculations were analyzed to present the effect of thermal stress. Typical rock properties were taken into consideration to demonstrate different assumptions. Table 3 shows several rock properties such as thermal expansion coefficient, elastic moduli, and Poisson's ratio.

Inputs presented in Table 3 were to simulate effect of thermal coefficient on wellbore stresses. Wellbore stresses versus thermal expansion coefficient were plotted in Fig. 12. It is seen that the higher thermal expansion coefficient can be the reason the lower hoop stress magnitude resulting fluid loss easily. However, radial stress changes with changing thermal coefficient due to the difference between wellbore and pore pressure.

Table 3. Some typical rock properties.

Rock type	Thermal expansion coefficient (1/°F)	Elastic Young's modulus (psi)	Poisson's ratio (frac)
Marble	1.84E-06	7.65E+06	0.25
Gneiss	2.11E-06	7.90E+06	0.24
Schist	7.97E-06	4.64E+06	0.2
Andesite	4.35E-06	5.80E+06	0.2
Granite	6.52E-06	7.25E+06	0.17
Slate	2.90E-06	7.97E+06	0.25
Sandstone	8.33E-06	4.35E+06	0.14
Limestone	3.62E-06	6.53E+06	0.3

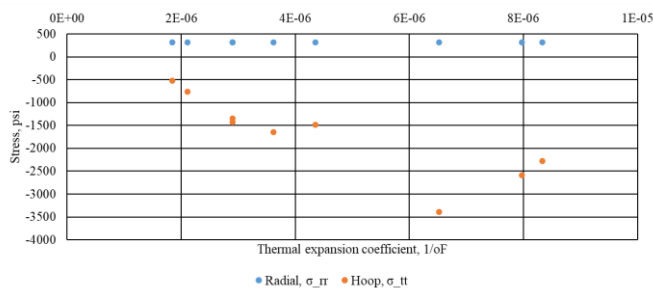


Figure 12. Thermal expansion variation on wellbore stresses.

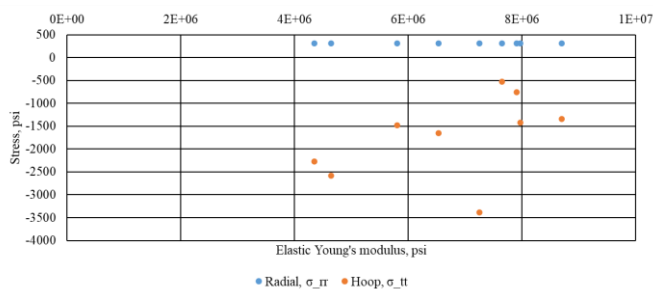


Figure 13. Elastic Young's modulus effects on stresses around the wellbore.

Fig. 13 shows the relationship between Elastic Young's modulus and stresses around the wellbore. Since Young's modulus determines the material stiffness, the greater Elastic modulus causes less magnitude of hoop stress, which means the low possibility of encountered fluid loss. It should be noted that the low magnitude of Elastic modulus can result in presenting more severe lost circulation cases due to carrying soft rock properties. Considering different rock properties means that each rock has different thermal expansion coefficient and Poisson's ratio. Therefore, Elastic Young's modulus on thermal effects do not behave a linear trend while observing stresses around the wellbore.

Poisson's ratio is another rock property we used to analyze to present its effects on wellbore stresses and lost circulation. Fig. 14 demonstrates the coupling between Poisson's ratio and stresses around the wellbore. If the Poisson's ratio magnitude is

high, the fluid loss phenomena are less likely to occur. Since Poisson's ratio determines the ratio of the deformation between the transverse and axial, the lower value results in the higher possibility of loss into the formation.

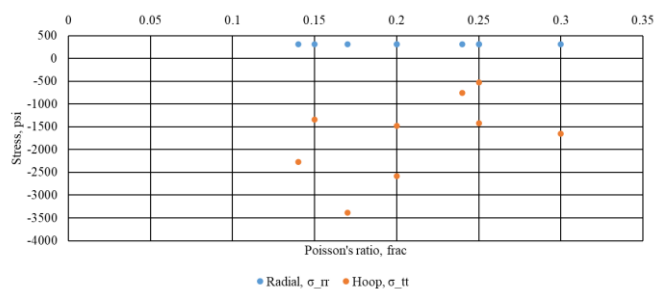


Figure 14. Effect of Poisson's ratio on wellbore stresses.

### **Electric Capacity of Reservoir**

Geothermal energy resources are evaluated to produce energy either for using direct thermal use or for electricity generation. However, due to deficiencies of reservoir properties, it is hard to recognize proper exploitation capacity. Since geothermal energy is considered renewable energy, it requires a throughout economical evaluation to determine if the economical benefits of the resource rock (Sanyal, 2005). Construction of large scale geothermal power plants has been observed through time, the new concept is to make it more sustainable with the reinjection process. The coupling between reservoir capacity and power plant parameters plays a vital role in deciding the power plant design.

Uncertainty analysis corresponds to obtaining a reliable result with Monte Carlo simulations to estimate electric power capacity for a geothermal system. According to USGS, the maximum and minimum temperature and volume are considered to obtain probability distributions. Thermodynamic laws help to observe the exergy of the system as a maximum functional approach during the well production. Uncertainty analysis works based on the most likely, mean, median, 5 percent, and 90 percent electric power capacity potential. For this study, a developed Monte Carlo uncertainty analysis study is implemented, including reservoir volume, reservoir temperature, and recovery factor (Williams et al., 2008).

Fig. 15 demonstrates optimum reservoir capacity conditions and clearly explains P5 and P95 values of 93.7 and 137.4 MWe, respectively. The estimated mean of energy is 112.98 MWe, which is the most likely value to obtain energy from the reservoir. Harnessing PML1 geothermal reservoir can help to generate 112-megawatt electricity that supplies approximately 112,000 households.

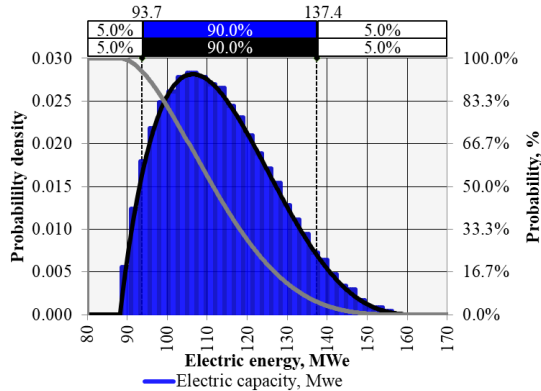


Figure 15. Electric energy capacity of PML1 reservoir.

## Conclusions

This paper presents a case study analysis of a geothermal well where fluid loss was encountered. The temperature distribution along with the wellbore and stress variation around the wellbore during fluid circulation is observed by integrating a failure criterion. The temperature distribution, stress alteration around the wellbore, and Mohr-Coulomb failure criterion are obtained using an analytical approach method. This paper covers an approach that results from solving fluid circulation through wellbore during lost circulation and stress deformation at a depth of fluid loss in a unique temperature condition. The following outcomes are observed by applying analytical solutions:

- The drilling fluid temperature plays an influential role in the occurrence of fluid loss. The cooler mud leads to a higher bottom-hole temperature change and results in tensile stress around the wellbore.
- The stresses around wellbore demonstrate that the hoop stress magnitude of -900 psi may cause tensile failure around the wellbore.
- The case study shows that the temperature differences of higher than 100 °F cause total loss without fluid circulation.
- This paper provides a consistent temperature estimation along the wellbore and implements failure criteria to obtain a more accurate instability analysis.
- The presence of marble around the borehole shows that a higher possibility of loss of circulation can be seen in the hard rock formation if the temperature difference is greater than 100 °F.

## Acknowledgments

Both Dr. Tan C. Nguyen and Dr. Arild Saasen have provided many useful insights into the research that have greatly influenced my thinking on the subject. The work reported in this paper was supported by the Republic of Turkey Ministry of National Education and the General Directorate of Mineral Exploration and Research that is gratefully acknowledged.

## Nomenclature

$S_v$	Vertical Stress, psi
$S_{Hmax}$	Maximum horizontal stress, psi
$S_{Hmin}$	Minimum horizontal stress, psi
$\sigma_{\theta\theta}$	Hoop or tangential stress, psi
$\sigma_{rr}$	Radial stress, psi
$\sigma_{aa}$	Axial stress, psi
$\tau_{r\theta}$	Shear stress, psi
$P_p$	Pore pressure, psi
$P_w$	Mud pressure, psi
$Q$	Heat flow, Btu/lbm
$c_m$	Specific heat of the mud, Btu/lbm-°F
$z$	Vertical depth, ft
$k$	Thermal conductivity, Btu/hr-ft-°F
$T_a$	Annulus temperature, °F
$T_{as}$	Drillstring temperature, °F
$g_G$	Geothermal gradient, °F/ft
$\phi$	Porosity, frac
$\mu$	Internal friction coefficient
$\varphi$	Friction angle, deg.
$C_0$	Unconfined compressive strength, psi
$E$	Elastic Young's modulus, psi
$\nu$	Poisson's ratio
$r_e$	Wellbore radius, ft
$r_t$	Drillstring radius, ft

## References

1. Al-Ajmi, A. M., & Zimmerman, R. W. (2005). Relation between the Mogi and the Coulomb failure criteria. *International Journal of Rock Mechanics and Mining Sciences*, 42(3), 431-439.
2. Al Saedi, A. Q. A. (2020). *Exploring wellbore and reservoir temperature profiles in fluid circulation and production operations*. Missouri University of Science and Technology.
3. Carson, C. C., & Lin, Y. (1982). *Impact of common problems in geothermal drilling and completion*.
4. Cole, P., Young, K., Doke, C., Duncan, N., & Eustes, B. (2017). Geothermal drilling: a baseline study of nonproductive time related to lost circulation. Proceedings of the 42nd Workshop on Geothermal Reservoir Engineering, Stanford, CA, USA.
5. Espinoza, N. (2020). Tensile Fractures and Wellbore Breakdown. <https://dnicolasespinoza.github.io/node46.html>
6. Fjær, E., Holt, R., Horsrud, P., Raaen, A., & Risnes, R. (2008). Reservoir geomechanics. *Developments in Petroleum Science*, 53, 391-433.

7. Handin, J., & Hager, R. V., Jr. (1957). Experimental Deformation of Sedimentary Rocks Under Confining Pressure: Tests at Room Temperature on Dry Samples1. *AAPG Bulletin*, 41(1), 1-50. <https://doi.org/10.1306/5ceae5fb-16bb-11d7-8645000102c1865d>
8. Hasan, A. R., & Kabir, C. (1994). Aspects of wellbore heat transfer during two-phase flow (includes associated papers 30226 and 30970). *SPE Production & Facilities*, 9(03), 211-216.
9. Holmes, C. S., & Swift, S. C. (1970). Calculation of circulating mud temperatures. *Journal of Petroleum Technology*, 22(06), 670-674.
10. Jaeger, J. C., Cook, N. G., & Zimmerman, R. (2009). *Fundamentals of rock mechanics*. John Wiley & Sons.
11. Kabir, C., Hasan, A., Kouba, G., & Ameen, M. (1996). Determining circulating fluid temperature in drilling, workover, and well control operations. *SPE Drilling & Completion*, 11(02), 74-79.
12. Loeppke, G. E., Glowka, D. A., & Wright, E. K. (1990). Design and evaluation of lost-circulation materials for severe environments. *Journal of Petroleum Technology*, 42(03), 328-337.
13. Raymond, L. (1969). Temperature distribution in a circulating drilling fluid. *Journal of Petroleum Technology*, 21(03), 333-341.
14. Sanyal, S. K. (2005). Cost of geothermal power and factors that affect it. Proceedings world geothermal congress,
15. Shaker Selim, S. (2008). *Loss of circulation: Causes and consequences in geopressured systems*.
16. Turcotte, D. L., & Schubert, G. (2002). *Geodynamics*. Cambridge university press.
17. Williams, C. F., Reed, M., & Mariner, R. H. (2008). *A Review of Methods Applied by the US Geological Survey in the Assessment of Identified Geothermal Resources*. Citeseer.
18. Zoback, M. D. (2010). *Reservoir geomechanics*. Cambridge university press.
19. Zoback, M. D., Barton, C. A., Brudy, M., Castillo, D. A., Finkbeiner, T., Grollimund, B. R., Moos, D. B., Peska, P., Ward, C. D., & Wiprut, D. J. (2003). Determination of stress orientation and magnitude in deep wells. *International Journal of Rock Mechanics and Mining Sciences*, 40(7-8), 1049-1076. <https://doi.org/10.1016/j.ijrmms.2003.07.001>